



ELSEVIER

Contents lists available at [SciVerse ScienceDirect](http://www.sciencedirect.com)

Comptes Rendus Chimie

www.sciencedirect.com



Full paper/Mémoire

Inclusion complexes of ortho-anisidine and β -cyclodextrin: A quantum mechanical calculation

Djilani Imene, Nouar Leila ^{*}, Madi Fatiha Haiahem Sakina, Bouhadiba Abdelaziz,
Khatmi DjamelEddine

Laboratory of computational chemistry and nanostructures, Department of material sciences, Faculty of mathematical, informatics and material sciences,
University of 08 Mai 1945, Guelma, Algeria

ARTICLE INFO

Article history:

Received 26 November 2012

Accepted after revision 11 February 2013

Available online xxx

Keywords:

Cyclodextrin
Ortho-anisidine
PM6
ONIOM2
NBO

ABSTRACT

The structural aspects for the complexation of ortho-anisidine (O-AN)/ β -cyclodextrin were explored by using PM6, density function theory B3LYP/6-31G*, M05-2X/6-31G*, B3PW91/6-31G*, MPW1PW91/6-31G*, HF/6-31G* methods and several combinations of ONIOM2 hybrid calculations. Calculations were performed upon the inclusion complexation of β -cyclodextrin (β -CD) with neutral (O-AN1) and cationic (O-AN2) species of ortho-anisidine. The obtained results with PM6 method clearly indicate that the formed complexes are energetically favored, the complex of O-AN2/ β -CD in B orientation is significantly more favorable than the others energetically. The structures show the presence of several intermolecular hydrogen bond interactions that were studied on the basis of natural bonding orbital (NBO) analysis, employed to quantify the donor–acceptor interactions between ortho-anisidine and β -CD.

© 2013 Académie des sciences. Published by Elsevier Masson SAS. All rights reserved.

1. Introduction

Cyclodextrins (CD) are cyclic oligosaccharides that present a hydrophilic external part and a relatively hydrophobic cavity in which guest molecules can be encapsulated by inclusion complex formation [1,2]. The most widely used (CDs) are α -, β - and γ (CDs). The ability of β -CD to form inclusion complexes with different products is well known. In particular, β -CD (Fig. 1a) has an internal cavity, shaped like a truncated cone of about 8 Å deep and 6.0–6.4 Å in diameter. This cavity possesses a relatively low polarity that can accommodate guest organic molecules inside. The formation of inclusion complexes of organic molecules with cyclodextrins is

important for their pharmaceutical and technological applications [3–6].

The applications of O-AN (Fig. 1b) in various fields like catalysis and chemicals processing, chemical synthesis, colorants for paper, dyestuffs, pigments and optical brighteners. In electrochemical synthesis of polymer material using the O-AN [7] to form thin films and composite material. O-AN used as reducing agent in gold nano particle preparation in aqueous solution. Formulation and practical application of O-AN are often rendered difficult due to their adverse physicochemical properties such as poor solubility, instability, toxicity, and volatility [8]. The complexation between O-AN and cyclodextrins can result in products with superior performance (e.g., enhanced OAN solubility and stability, reduction of volatility).

Srinivasan et al. [9] prepared and characterized by XRD, SEM and FT-IR techniques, the solid complex of both species (neutral and cationic) of O-AN with β -CD. The

^{*} Corresponding author.

E-mail address: leilanoua@yahoo.fr (N. Leila).

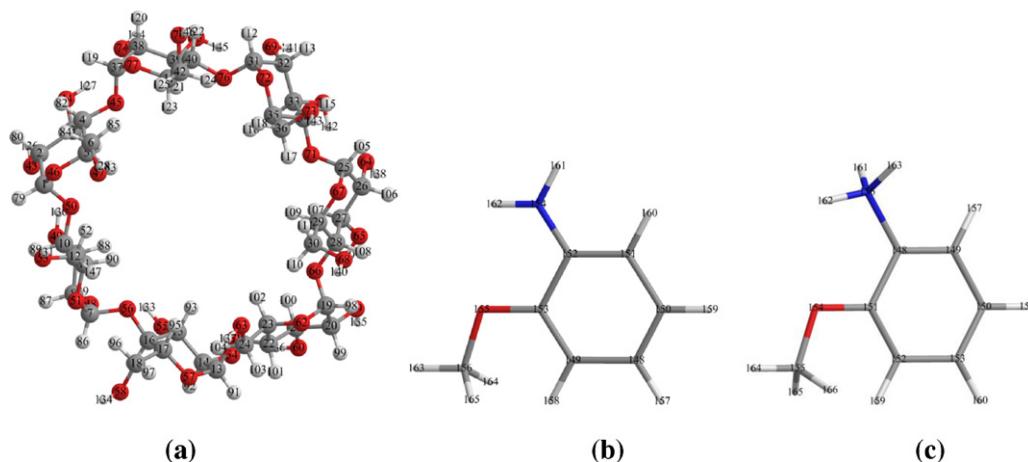


Fig. 1. Geometrical structures of β -CD (a), neutral (b) and cationic (c) species of O-AN optimized at PM6 method.

results indicate that the O-AN molecule is entrapped in the β -CD cavity to form an inclusion complex. The thermodynamic parameters in this inclusion process show that the reaction of β -CD with both species of O-AN is exothermic and accompanied with a negative entropy (ΔS).

Recently, the new semi-empirical method PM6 (parameterized model 6) was introduced [10–14], which is superior to other semi-empirical QM methods in various aspects. As compared to the earlier semi-empirical methods AM1 and PM3, several modifications have been made to the neglect of diatomic differential overlap (NDDO) core-core interaction term and to the parameter optimization method.

In this study, the complexation and deformation energies of both β -CD and O-AN during the formation of inclusion complexes were studied, using PM6 semi-empirical method in order to localize the minimum energy structures, which are used as starting structures for subsequent optimizations. After that, the structures are subjected to higher-level calculations, such HF, DFT and ONIOM2 methods to approach the ideal geometry and provide further insight into the complexation process of O-AN with β -CD. Furthermore, the natural bonding orbital (NBO) analysis is employed to quantify the donor–acceptor interactions between host and guest.

2. Computational method

In this study, we have considered only the inclusion compounds in molar proportion 1:1 formed between one molecule of β -CD and one of O-AN, abbreviated O-AN1/ β -CD (A), O-AN1/ β -CD (B), O-AN2/ β -CD (A) and O-AN2/ β -CD (B), (1 and 2 represent neutral and cationic species of O-AN respectively).

The initial structures of the cationic and the neutral species of O-AN were constructed using Hyperchem 7.5 molecular modeling package [15]. The starting geometry of β -CD was taken from Chem-Office 3D ultra (version10, Cambridge software). The two structures O-AN and β -CD were then optimized by means of PM6 semi-empirical

method prior to using Gaussian09 [16] for all relevant calculations.

The inclusion model is shown in Fig. 2. It contains one passing process and one circling process.

For the construction of O-AN/ β -CD complex, the glycosidic oxygen atoms of the cyclodextrin molecule were placed on the XY plane and their center was defined as the center of the coordinate system. The secondary hydroxyl groups of the β -CD were placed pointing toward the positive Z axis. The hydroxyl group of the guest molecule was initially placed along the Z axis. Two possible orientations of the guest molecule in the complex were considered. The orientation in which the hydroxyl group of O-AN points toward the secondary hydroxyl of β -CD was called the “A orientation”, the other, in which the hydroxyl group of the guest points toward the primary hydroxyl of β -CD was called the “B orientation”, (Fig. 2).

The relative position between the host and the guest was measured by the Z-coordinate of the labeled carbon atom (C^*) of the guest (Fig. 2). The inclusion process emulation was then achieved along the Z axis from 10 to -10 Å with a step of 1 Å. The generated structures at each step were optimized by PM6 methods without imposing any symmetrical restrictions.

In order to find an even more stable structure of the complex, each guest molecule is calculated for all of the structures obtained by scanning θ , clock wisely circling around Z-axis, at 30° intervals from 0° to 360° .

Complexation energy upon complexes between O-AN and the β -CD is calculated for the minimum energy structure according to Eq. (1).

$$\Delta E = E_{\text{complex}} - (E_{\text{free O-AN}} + E_{\text{free } \beta\text{-CD}}) \quad (1)$$

where E_{complex} , $E_{\text{free } \beta\text{-CD}}$ and $E_{\text{free O-AN}}$ represent respectively the total energy of the complex, the free optimized β -CD and the free optimized O-AN energy. The magnitude of the energy change would be a metric of the driving force toward complexation.

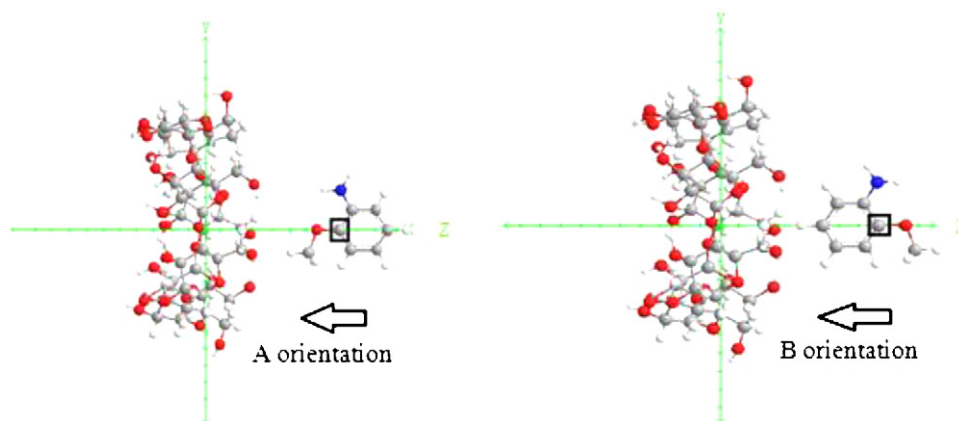


Fig. 2. Coordinate systems to describe inclusion processes of O-AN with β -CD.

The deformation energy for each component, the guest or the host molecule, throughout the formation of the complex, was defined as the difference in the energy of the totally optimized component compared to its energy in the complex as Eq. (2)

$$E_{\text{deformation}}(\text{component}) = E[\text{component}]_{\text{sp}}^{\text{opt}} - E[\text{component}]_{\text{opt}} \quad (2)$$

For the purpose of this work, the B3LYP [17–22] and B3PW91 [23–27] density functional were employed as they are the most widely used density functional and the most popular. In addition to the above-mentioned functional, we have also used the Minnesota density M05-2X functional, a member of the M05 families of density functionals developed by Zhao, Truhlar and Schultz, which gave good results [28,29] and is beginning to be increasingly used [30–32], and which gives us a good result in our study of the O-AN/ β -CD complex.

3. Results and discussion

3.1. Passing and circling process

The graphical representation of the energy changes involved during the inclusion passing process of O-AN in

β -CD at different Z positions for both orientations are illustrated in Fig. 3.

The first remark is that all complexation energies are negative, which show that the inclusion process of O-AN in β -CD is thermodynamically favorable. Second, the curves show several local minima, where the lowest minimum energy is precisely located at Z value of -6 \AA and 0 \AA respectively for neutral and cationic species of O-AN for the A orientation. The energy minimum for the B orientation is located at Z values of -3 \AA and 1 \AA respectively for neutral and cationic species of O-AN.

We can also notice that the lowest energy is obtained when θ is equal to 330° and 210° respectively for neutral and cationic species of O-AN for A orientation, but for the B orientation, it is located at 0° and 60° respectively for neutral and cationic species of O-AN. The energy changes of 1 and 2 complexes are exhibited in Fig. 4.

3.2. The optimization

The calculated energies for the most stable structures obtained by PM6 study are summarized in Table 1. The values of the energy minimum for both A orientation and B orientation in anionic and cationic forms are respectively equal to -13.20 , -13.50 , -35.13 and -35.51 kcal/mol,

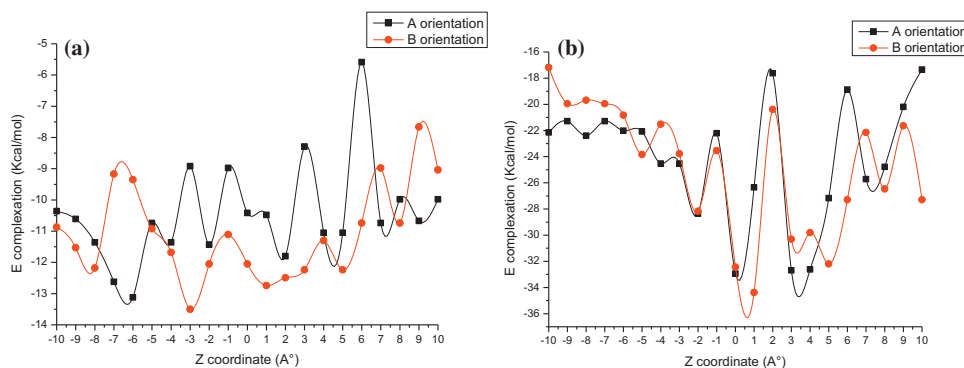


Fig. 3. Binding energies of the inclusion complexation of O-AN1/ β -CD (a) and O-AN2/ β -CD (b) at different positions (Z) and for both orientations.

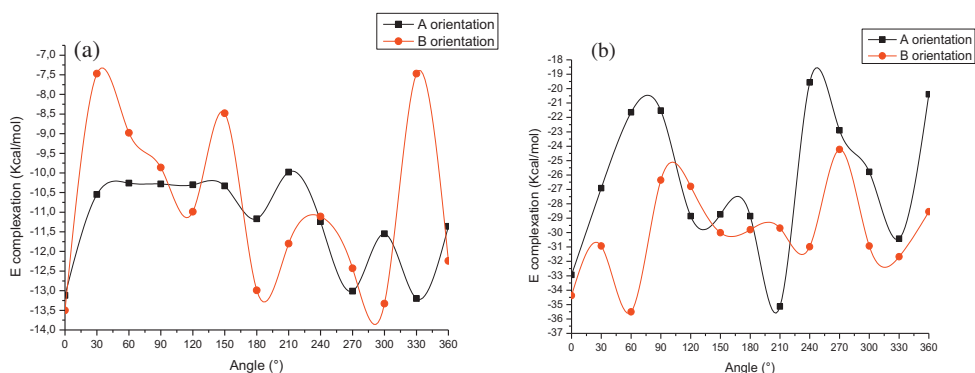


Fig. 4. Stability energies of the inclusion complexation of O-AN1/ β -CD (a) and O-AN2/ β -CD (b) at different angles (θ), PM6 calculations.

which indicates that the complexation energy is slightly in favor of the B orientation in cationic form. This weak difference in the complexation obtained with PM6 does not allow determining the nature of the driving forces and their relative contributions. So, we did consider a higher level of calculation.

The gap energetic between the two orientations for neutral and cationic species of O-AN obtained with PM6 is increased using single point calculations at B3LYP/6-31G*, M05-2X/6-31G*, B3PW91/6-31G*, MPW1PW91/6-31G* and HF/6-31G* levels and confirm the preference for the

B orientation (O-AN2/ β -CD) over the other three complexes (Table 1).

The results of the investigation of deformation energy reported in Table 1 show that the cationic form of O-AN molecule for orientation B requires slightly more energy than for orientation A (in neutral and cationic species) in order to adapt its structure to bind within the cavity of β -CD as indicated by the DEF [O-AN] of about 11.28 kcal/mol. This can be supported by the fact that flexibility of the guest structure is an important structural requirement for β -CD upon complexation.

Table 1

Thermodynamic parameters of the complexes A and B for neutral and cationic O-AN calculated by PM6 method.

	O-AN	O-AN+1	β -CD	O-AN1/ β -CD		O-AN2/ β -CD	
				A	B	A	B
PM6							
E (kcal/mol)	-14.05	127.38	-1564.63	-1591.88	-1592.18	-1472.38	-1472.76
ΔE (kcal/mol)				-13.20	-13.50	-35.13	-35.51
$E_{\text{deformation}}$ (O-AN1)	-	-	-	14.02	12.93	-	-
$E_{\text{deformation}}$ (O-AN2)	-	-	-	-	-	11.63	11.28
$E_{\text{deformation}}$ (β -CD)	-	-	-	8.79	11.73	11.29	13.91
H^\ddagger (kcal/mol)	75.30	226.53	-834.58	-774.59	-774.84	-649.03	-649.15
ΔH^\ddagger (kcal/mol)				-15.31	-15.56	-40.98	-41.10
G^\ddagger (kcal/mol)	50.20	199.92	-941.26	-913.34	-914.59	-786.89	-787.58
ΔG^\ddagger (kcal/mol)				-22.28	-23.53	-45.55	-46.24
S^\ddagger (kcal/mol)	90.49	89.28	404.01	466.37	464.84	462.39	460.92
ΔS^\ddagger (kcal/mol)				-28.13	-29.66	-28.49	-29.96
B3LYP/6-31G*							
E (kcal/mol)	-252334.19	-252564.24	-2682649.17	-2934990.65	-2934997.74	-2935237.07	-2935239.76
ΔE (kcal/mol)				-7.29	-14.38	-23.66	-26.35
M05-2X/6-31G*							
E (kcal/mol)	-252300.93	-252528.66	-2682441.34	-2934744.22	-2934755.02	-2934987.57	-2934990.77
ΔE (kcal/mol)				-1.95	-12.75	-17.57	-20.77
MPW1PW91/6-31G*							
E (Kcal/mol)	-252259.02	-252503.05	-2682040.49	-2934312.50	-2934315.52	-2934558.29	-2934560.86
ΔE (kcal/mol)				-12.99	-16.01	-14.75	-17.32
B3PW91/6-31G*							
E (kcal/mol)	-252215.09	-252468.85	-2681667.62	-2933890.06	-2933895.58	-2934145.10	-2934151.29
ΔE (kcal/mol)				-7.35	-13.87	-8.63	-14.82
HF/6-31G*							
E (kcal/mol)	-250721.62	-250985.48	-2667563.83	-2918294.99	-2918303.97	-2918562.21	-2918568.54
ΔE (kcal/mol)				-9.54	-18.52	-12.90	-19.23

Table 2
Mulliken charges of the atoms of O-AN1 and O-AN2, charge transfer of the A and B orientations calculated by PM6//B3LYP/6-31G* method.

	O-AN	O-AN1/ β -CD		O-AN+1	O-AN2/ β -CD	
		A	B		A	B
C ₁₄₈	-0.040//−0.037	0.021//−0.035	0.058//−0.012	−0.305//0.111	−0.224//0.145	−0.230//0.164
C ₁₄₉	−0.067//−0.075	−0.091//−0.031	−0.092//−0.038	0.146//0.028	0.144//0.001	0.143//0.018
C ₁₅₀	0.047//−0.015	−0.005//0.007	−0.046//−0.025	−0.032//0.052	−0.060//0.014	−0.060//−0.007
C ₁₅₁	−0.144//−0.088	−0.027//−0.055	−0.011//−0.035	0.377//0.420	0.348//0.409	0.350//0.360
C ₁₅₂	0.201//0.323	0.064//0.227	0.032//0.220	−0.135//0.005	−0.148//−0.048	−0.120//0.031
C ₁₅₃	0.136//0.334	0.202//0.345	0.214//0.354	0.229//0.074	0.201//0.044	0.181//0.030
N ₁₅₄	0.011//−0.162	−0.012//−0.139	−0.017//−0.147	−0.405//−0.569	−0.409//−0.566	−0.400//−0.304
O ₁₅₅	−0.394//−0.550	−0.404//−0.560	−0.402//−0.559	0.330//0.356	0.317//0.319	0.320//0.295
C ₁₅₆	0.250//0.272	0.269//0.263	0.281//0.287	0.793//0.520	0.765//0.420	0.775//0.448
Somme	0.000//0.000	0.016//0.022	0.017//0.045	1.000//1.000	0.934//0.738	1.079//1.018

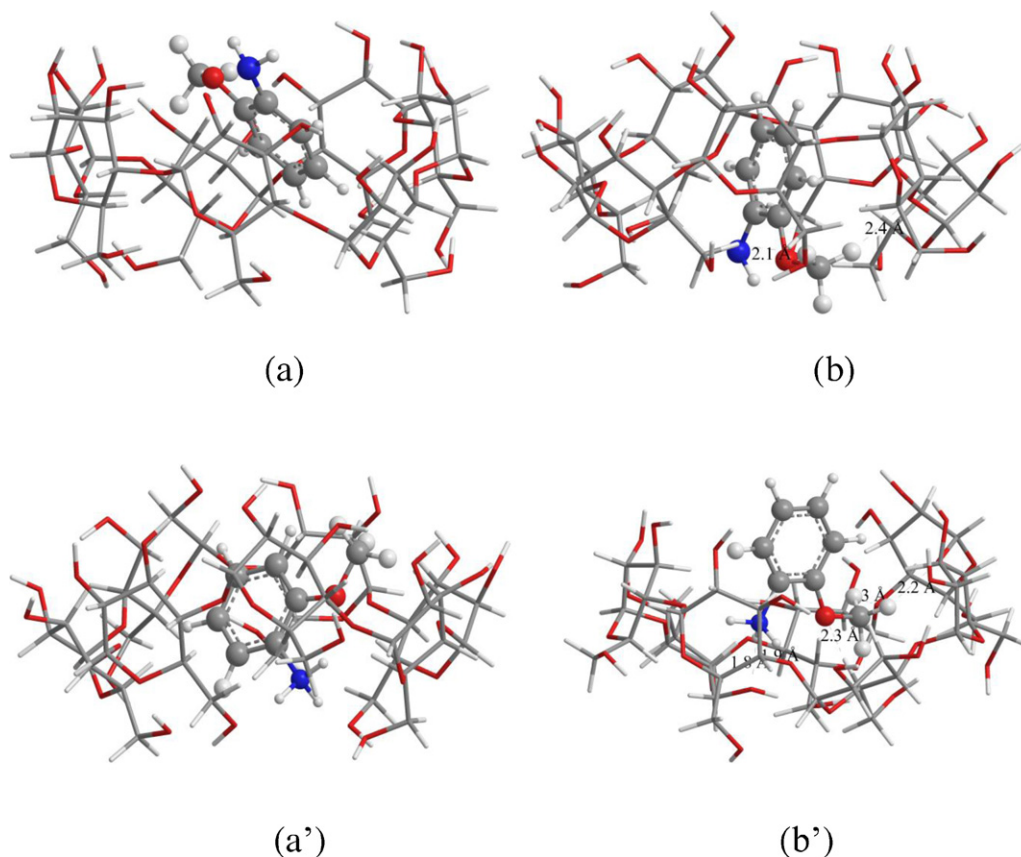
3.3. Thermodynamics parameters

The statistical thermodynamic calculation was carried out at 1 atm pressure and 298.15 K temperature by PM6 method. The thermodynamic quantities the enthalpy changes (ΔH), Gibbs energy changes (ΔG) and entropy changes (ΔS) contributions are depicted in Table 1. As can be seen from Table 1, ΔG is negative which suggests that the inclusion process proceeded spontaneously at 298K. ΔH and ΔS are also negative, which indicates that the inclusion process is an exergonic and enthalpy-controlled process. The negative enthalpy change (ΔH) arose from the

van der Waal's interaction, while the negative entropy change (ΔS) is the steric barrier caused by molecular geometrical shape and the limit of β -CD cavity to the freedom of shift and rotation of O-AN molecule. The same results are also given with the experimental observation [9].

3.4. Charge transfer

Liu and Guo suggest that charge-transfer interactions play a relevant role in the stabilization of their inclusion complexes [33]. The Mulliken charges of the heavy atoms

**Fig. 5.** ONIOM2 energy minimized structure of the O-AN1/ β -CD A (a), O-AN1/ β -CD B (b), O-AN2/ β -CD A (a') and O-AN2/ β -CD B (b'). Top view. Hydrogen bonds are indicated by dotted lines.

of O-AN1 and O-AN2, charge transfer of complexes O-AN1/ β -CD and O-AN2/ β -CD are summarized in Table 2 by B3LYP/6-31G* and PM6 methods. The data show that the β -CD molecule accepts the electron from O-AN and the charge transfer of O-AN2/ β -CD in B orientation (PM6: **1.079e**, B3LYP/6-31G*: **1.018e**) is the largest of all complexes.

For the O-AN1/ β -CD complex, Mulliken charge distribution indicates that there is a small but non-trivial transferred charge. The amount of this charge is pretty similar in both A and B orientation. Hence, in spite of that charge–transfer interaction, is a non-trivial driving force in the complexation of O-AN1 and β -CD, the stability of the A orientation in relation to the B one is not necessary assessed by this interaction [34,35].

3.5. The structure parameters of inclusion complexes

Among the structures of the four inclusion complexes shown in Fig. 5, we could notice that O-AN2/ β -CD in B orientation presents several intermolecular H-bonds in the structure. Here, the H-bond is defined as C–H–O or O–H–O and the N–H–O H bond lengths are less than 3 Å, which is in agreement with the reported data [36]. Obviously, the hydrogen bonds of O-AN2/ β -CD are more than those of the other three. This explains why the complexation energy of

the inclusion O-AN2/ β -CD in B orientation is lower than the other three complexes.

Table 3 presents the most interesting bond distances, bond angles and dihedral angles of the O-AN before and after complexation in β -CD obtained from PM6 and B3LYP/6-31G* calculations for the most stable structure (Fig. 5). It was evident that after complexation, the conformation of O-AN was completely altered. The alterations were significant in dihedral angles, which indicated that the O-AN adopted a specific conformation to form a stable complex.

3.6. ONIOM calculations

In order to further understand molecular recognition between the guest and the host, we adopted ONIOM2 methods. In our hybrid model study, we submitted the host molecule β -CD to the low level of quantum calculations (PM6) since we assumed it provides only an environmental effect and contains the larger number of atoms, while the guest molecule O-AN (neutral and cationic species) is treated at a high level of calculation HF/6-31G*, B3LYP/6-31G*, M05-2X/6-31G* and MPW1PW91/6-31G*. Table 4 emphasizes the computational results of the ONIOM2 study. It is interesting to note that the results indicate that the complexation according to the B

Table 3

Geometrical parameters of O-AN1 and O-AN2 before and after inclusion in β -CD, bond distances (Å), angle (°) and dihedral angles (°) calculated by PM6//B3LYP/6-31G* methods.

	O-AN 1	O-AN2	O-AN1/ β -CD		O-AN2/ β -CD	
			A	B	A	B
	PM6//B3LYP/6-31G*		PM6//B3LYP/6-31G*		PM6//B3LYP/6-31G*	
Bond lengths (Å)						
C ₁₄₈ –C ₁₄₉	1.408//1.408	1.0390//1.389	1.399//1.399	1.402//1.402	1.394//1.394	1.392//1.392
C ₁₄₉ –C ₁₅₃	1.384//1.384	1.405//1.405	1.393//1.393	1.392//1.392	1.401//1.401	1.402//1.402
C ₁₄₉ –H ₁₅₈	1.085//1.085	1.091//1.091	1.093//1.093	1.088//1.088	1.089//1.089	1.100//1.100
C ₁₅₀ –H ₁₅₉	1.088//1.088	1.094//1.094	1.091//1.091	1.089//1.089	1.102//1.102	1.091//1.091
C ₁₅₂ –C ₁₅₃	1.437//1.437	1.414//1.414	1.423//1.423	1.427//1.427	1.414//1.414	1.415//1.415
C ₁₅₂ –N ₁₅₄	1.392//1.392	1.478//1.478	1.432//1.432	1.427//1.427	1.474//1.474	1.475//1.475
C ₁₅₃ –O ₁₅₅	1.389//1.389	1.364//1.364	1.392//1.392	1.386//1.386	1.368//1.368	1.365//1.365
N ₁₅₄ –H ₁₆₁	0.997//0.997	1.034//1.034	1.033//1.033	1.025//1.025	1.051//1.051	1.044//1.044
N ₁₅₄ –H ₁₆₂	1.002//1.002	1.041//1.041	1.023//1.023	1.019//1.019	1.047//1.047	1.053//1.503
Bond angles (°)						
C ₁₄₉ –C ₁₄₈ –C ₁₅₀	120.305//120.302	120.894//120.897	120.520//120.520	120.355//120.355	120.763//120.761	120.991//120.991
C ₁₄₉ –C ₁₄₈ –H ₁₅₇	119.171//119.172	119.813//119.814	119.525//119.525	119.447//119.447	119.814//119.813	119.536//119.532
C ₁₅₀ –C ₁₄₈ –H ₁₅₇	120.526//120.526	119.292//120.288	119.977//119.977	120.197//120.197	119.416//119.419	119.473//119.477
C ₁₄₈ –C ₁₅₀ –H ₁₅₉	120.151//120.151	119.331//119.332	120.765//120.765	120.160//120.160	119.784//119.781	119.622//119.619
C ₁₅₀ –C ₁₅₁ –H ₁₆₀	119.684//119.684	120.243//120.241	120.361//120.361	119.806//119.806	120.342//120.345	120.265//120.265
C ₁₅₂ –C ₁₅₁ –H ₁₆₀	120.234//120.234	120.446//120.441	119.289//119.289	119.727//119.727	120.471//120.465	120.189//120.185
C ₁₅₁ –C ₁₅₂ –N ₁₅	121.991//121.991	120.499//120.501	119.601//119.601	120.391//120.391	120.519//120.519	121.375//121.375
Dihedral angle (°)						
C ₁₅₀ –C ₁₄₈ –C ₁₄₉ –C ₁₅	0.000//0.000	0.000//0.000	0.827//0.827	–0.304//–0.304	1.520//1.524	0.320//0.317
C ₁₅₀ –C ₁₄₈ –C ₁₄₉ –H ₁₅₈	–180.000//	180.000//180.000	–178.695//	178.998//178.998	–179.142//	–179.739//
	–180.000		–178.695		–179.143	–179.739
H ₁₅₇ –C ₁₄₈ –C ₁₄₉ –C ₁₅₃	0.000//–180.000	0.000//–180.000	–179.074//	–179.917//	–177.498//	–179.831//
			–179.074	–179.917	–177.496	–179.829
C ₁₄₉ –C ₁₄₈ –C ₁₅₀ –C ₁₅₁	0.000//0.000	0.000//0.000	–0.937//–0.937	0.556//0.556	–0.898//–0.899	0.031//0.032
C ₁₄₉ –C ₁₄₈ –C ₁₅₀ –H ₁₅₉	–180.000//	180.000//180.000	179.732//179.732	–179.512//	178.817//178.816	–179.873//
	–180.000			–179.512		–179.873
H ₁₅₇ –C ₁₄₈ –C ₁₅₀ –C ₁₅₁	180.000//0.000	180.000//	178.964//178.964	–179.833//	178.23//178.125	–179.818//
		–180.000		–179.833		–179.823
C ₁₄₈ –C ₁₄₉ –C ₁₅₃ –C ₁₅₂	0.000//0.000	0.000//0.0000	1.046//1.046	–0.641//–0.641	–0.796//–0.800	–0.355//
						–0.352

Table 4Relative energy for the optimized structures of complexes O-AN1/ β -CD and O-AN2/ β -CD in both orientations as calculated by ONIOM2 method.

	O-AN1/ β -CD			O-AN2/ β -CD		
	A	B	ΔE	A	B	ΔE
E (PM6)	-1591.88	-1592.18	-0.30	-1472.38	-1472.76	-0.38
E_{ONIOM} (B3LYP/6-31G*:PM6)	-253912.57	-253913.17	-0.60	-254165.70	-254165.96	-0.26
E_{ONIOM} (M05-2X/6-31G*:PM6)	-253879.69	-253880.19	-0.50	-254130.88	-254131.28	-0.40
E_{ONIOM} (MPW1PW91/6-31G*:PM6)	-253851.89	-253852.26	-0.37	-254105.21	-254105.40	-0.19
E_{ONIOM} (HF/6-31G*:PM6)	-252334.58	-252335.07	-0.49	-252590.03	-252590.53	-0.50

Table 5Donor–acceptor interactions and stabilization energies $E^{(2)}$ (kcal/mol).

β -CD donor O-AN acceptor	$E^{(2)}$ B3LYP/6-31G*	$E^{(2)}$ M05-2X/6-31G*	$E^{(2)}$ MPW1PW91/6-31G*	$E^{(2)}$ HF/6-31G*	
<i>B orientation for cationic O-AN</i>					
δ (1) C 15 - H 93	$\delta^*(1)$ C 155 - H 165	3.01	3.10	3.04	2.87
δ (1) O 53 - H 131	$\delta^*(1)$ C 155 - H 164	1.85	1.75	1.78	1.74
LP (1) O 47	$\delta^*(1)$ N 156 - H 161	1.67	1.62	1.69	1.32
LP (1) O 54	$\delta^*(1)$ C 152 - H 159	1.40	1.68	1.42	1.68
LP (1) O 56	$\delta^*(1)$ C 155 - H 165	1.78	1.78	1.74	1.90
LP (1) O 61	$\delta^*(1)$ C 155 - H 166	2.12	2.34	2.09	2.28
LP (1) O 71	$\delta^*(1)$ N 156 - H 162	3.94	3.37	3.24	3.00
<i>O-AN donor β-CD acceptor</i>					
<i>B orientation for cationic O-AN</i>					
δ (1) C 151 - H 160	$\delta^*(1)$ C 41 - H 123	4.19	4.12	4.18	4.02
δ (1) C 156 - H 165	$\delta^*(1)$ C 30 - H 110	1.78	1.90	1.90	1.48
LP (1) N 154	$\delta^*(1)$ C 12 - H 52	1.39	1.44	1.39	1.39
LP (1) N 154	$\delta^*(1)$ C 36 - H 118	2.45	2.51	2.45	2.44

orientation in cationic species is significantly more favorable than the other three complexes. ONIOM2 calculations confirm PM6 results.

Furthermore, it can be seen that the gap of the complexation energy between the two orientations in the four calculations vary considerably to -0.37 at -0.60 kcal/mol and -0.19 at -0.50 kcal/mol respectively in neutral and cationic species of O-AN. The more stable complex is obtained with [(B3LYP/6-31G*:PM6)] and [(HF/6-31G*:PM6)] level.

3.7. Natural Bond Orbital (NBO) analysis

NBO analysis provides an efficient method for studying intra- and intermolecular bonding and interaction between bonds, and also provides a convenient basis for investigating charge transfer or conjugative interaction in molecular systems. Some electron donor orbital, acceptor orbital and the interacting stabilization energy resulted from the second-order micro-disturbance theory are reported [37,38]. The second-order Fock matrix was carried out to evaluate the donor–acceptor interactions in the NBO analysis [39]. For each donor (i) and acceptor (j), the stabilization energy $E^{(2)}$ associated with the delocalization $i \rightarrow j$ is estimated as:

$$E^{(2)} = AE_{ij} = \frac{q_i F(i,j)}{\varepsilon_j - \varepsilon_i} \quad (3)$$

where q_i is the donor orbital occupancy, ε_i and ε_j are diagonal elements and $F(i,j)$ is the off diagonal NBO Fock

matrix element [40]. The electron donor orbital, electron acceptor orbital, and their corresponding $E^{(2)}$ energies for the B orientation in cationic form are shown in Table 5

From Table 5, it can be seen that a great number of donor σ C–H or σ N–H and acceptor $\sigma^* \text{C–H}$ interactions occur between the cavity and the guest molecule. The interactions energies of these contacts are in the range of 1.32–4.19 kcal/mol. The interactions are in detail:

- when O-AN plays the role of acceptor, the important interaction is observed between LP (O 71) and $\sigma^* \text{N 156 - H 162}$ (3.94 kcal/mol from B3LYP/6-31G* calculations);
- vacant orbital $\sigma^* \text{C–H}$ of β -CD accepts donor σ C–H from guest molecule, where the greater interaction is formed between σ C 151 - H 160 and $\sigma^* \text{C 41 - H 123}$ (4.19 kcal/mol from B3LYP/6-31G* calculations).

4. Conclusions

The stable structures and the inclusion process for neutral (O-AN1) and anionic (O-AN2) species of ortho-anisidine (O-AN)/ β -cyclodextrin inclusion complexes were studied by use of PM6, DFT, HF methods and several combinations of ONIOM2 hybrid calculations.

The result suggests that the complexation energy of the O-AN2/ β -CD in B orientation is significantly more favorable than the others. The statistical thermodynamic calculations suggest that the formation of the inclusion of β -CD with neutral and cationic species of O-AN was an exothermic reaction accompanied with negative ΔS . In addition, NBO analysis gives that mutual interactions

between donor and acceptor orbital of each O-AN and β -CD plays an important role to the stabilization of such complex.

The solvent effect that is not considered in this study plays probably an important role of complexation between O-AN and cyclodextrins. Nevertheless, the present work represents a preliminary result, which gives an idea of the inclusion process of O-AN in CDs.

Acknowledgments

This study was supported by the Algerian Ministry of Higher Education and Scientific Research and the General Direction of Scientific Research as a part of projects CNEPRU (No. **B01520090002**) and PNR (**8/u24/4814**).

References

- [1] O.K. Abou-Zied, A.T. Al-Hinai, J. Phys. Chem. 110 (2006) 7835.
- [2] J. Szejtli, Chem. Rev. 98 (1998) 1743.
- [3] M.V. Rekharsky, Y. Inoue, Chem. Rev. 98 (1998) 1875.
- [4] K.B. Lipkowitz, Chem. Rev. 98 (1998) 1829.
- [5] R.K. Sankaranaryanan, S. Siva, A. Antony Muthu Prabu, N. Rajendiran, J. Mol. Liq. 161 (2011) 107.
- [6] G. Venkatesh, A. Antony Muthu Prabu, N. Rajendiran, J. Fluoresc. 21 (2011) 1485.
- [7] S. Patil, J.R. Mahajan, M.A. More, P.P. Patil, S.W. Gosavi, S.A. Gangal, Poly. Inter. 46 (1998) 99.
- [8] P. Bertinello, A. Notargiacomo, D.J. Rile, M.K. Ram, C. Nicolini, Electrochem. Commun. 5 (2003) 787.
- [9] K. Srinivasan, J. Vaheethabanu, P. Manisankar, T. Stalin, J. Mol. Struct. 987 (2011) 214.
- [10] J. James, P. Stewart, J. Mol. Model. 13 (2007) 1173.
- [11] J. Rezac, J. Fanfrlik, D. Salahub, P. Hobza, J. Chem. Theory Comput. 5 (2009) 1749.
- [12] M.V. Gaspar de Araujo, O.F.L. Macedo, C. da Cunha Nascimento, L.S. Conegero, L.S. Barreto, L.E. Almeida, N. Bezerra da Costa Jr., I.F. Gimenez, Spectrochim. Acta A Mol. Biomol. Spectrosc. 72 (2009) 165.
- [13] M.V. Gaspar de Araújo, E.K. Barbosa Vieira, G.S. Lázaro, L.S. Conegero, L.E. Almeida, L.S. Barreto, N. Bezerra da Costa Jr., I.F. Gimenez, Bioorg. Med. Chem. 16 (2008) 5788.
- [14] X. Yong, W. Xueye, Y. Zhang, L. Benhua, Comput. Theor. Chem. 967 (2011) 213.
- [15] Hyperchem, Release 7.51 for windows 2002 Hypercube. Inc.
- [16] M.J. Frisch, G.W. Trucks, H.B. Schlegel, G.E. Scuseria, M.A. Robb, J.R. Cheeseman, G. Scalmani, V. Barone, B. Mennucci, G.A. Petersson, H. Nakatsuji, M. Caricato, X. Li, H.P. Hratchian, A.F. Izmaylov, J. Bloino, G. Zheng, J.L. Sonnenberg, M. Hada, M. Ehara, K. Toyota, R. Fukuda, J. Hasegawa, M. Ishida, T. Nakajima, Y. Honda, O. Kitao, H. Nakai, T. Vreven, J.A. Montgomery Jr., J.E. Peralta, F. Ogliaro, M. Bearpark, J.J. Heyd, E. Brothers, K.N. Kudin, V.N. Staroverov, R. Kobayashi, J. Normand, K. Raghavachari, A. Rendell, J.C. Burant, S.S. Iyengar, J. Tomasi, M. Cossi, N. Rega, J.M. Millam, M. Klene, J.E. Knox, J.B. Cross, V. Bakken, C. Adamo, J. Jaramillo, R. Gomperts, R.E. Stratmann, O. Yazyev, A.J. Austin, R. Cammi, C. Pomelli, J.W. Ochterski, R.L. Martin, K. Morokuma, V.G. Zakrzewski, G.A. Voth, P. Salvador, J.J. Dannenberg, S. Dapprich, A.D. Daniels, O. Farkas, J.B. Foresman, J.V. Ortiz, J. Cioslowski, D.J. Fox, Gaussian, Inc. Wallingford CT, 2009.
- [17] J.J.P. Stewart, J. Mol. Model. 14 (2008) 499.
- [18] M. Juan, B. Giussi, A. Gastaca, M.S. Albesa, P.E. Cortizo, Allegretti, Spectrochim. Acta A Mol. Biomol. Spectrosc. 78 (2011) 868.
- [19] K. Morokuma, Bull. Korean Chem. Soc. 24 (6) (2003) 797.
- [20] M.J. Huang, Z. Quan, Y.M. Liu, Int. J. Quantum Chem. 109 (1) (2009) 81.
- [21] A.D. Becke, J. Chem. Phys. 98 (1993) 5648.
- [22] W. Li, L. Bitai, F. Chen, F. Yang, Z. Wang, J. Mol. Struct. 990 (2011) 244.
- [23] S. Ramalingama, S. Perianthy, Spectrochim. Acta A 78 (2011) 1149.
- [24] L. Liu, H. Gao, Spectrochim. Acta A. 89 (2012) 201.
- [25] B.G. Willis, K.F. Jensen, J. Phys. Chem. A 102 (1998) 2613.
- [26] M.S. Sadjadi, B. Sadeghi, K. Zare, J. Mol. Struct. 817 (2007) 27.
- [27] A.F. Jalbout, F. Nazari, L. Turker, Gaussian-based computations in molecular science, J. Mol. Struct. 671 (2004) 1.
- [28] K. Helios, R. Wysokiński, A. Pietraszko, D. Michalska, Vibrational Spectrosc. 55 (2011) 207.
- [29] J. Gu, J. Wang, J. Leszczynski, Chem. Phys. Lett. 512 (2011) 108.
- [30] Y. Li, W. Guo, W. Fan, Z. Qin, J. Wang, Chin. J. Catal. 31 (2010) 1419.
- [31] Y. Zhao, N.E. Schultz, D.G. Truhlar, J. Chem. Theory Comput. 2 (2006) 364.
- [32] Y. Zhao, D.G. Truhlar, J. Chem. Theory Comput. 3 (2007) 289.
- [33] L. Liu, K.S. Song, L.I. Xiao-Song, G. Qing-Xiang, J. Incl. Phenom. Macrocycl. Chem. 40 (2001) 35–39.
- [34] L. Liu, K.S. Song, X.S. Li, Q.X. Guo, J. Incl. Phenom. Macrocycl. Chem. 40 (2001) 35.
- [35] A.D. Sayede, A. Ponchel, G. Filardo, A. Galia, E. Monflier, J. Mol. Struct. 777 (2006) 99.
- [36] H. Aki, T. Niiya, Y. Iwase, Y. Kawasaki, K. Kumai, T. Kimura, Thermochim. Acta 416 (2004) 87.
- [37] C. James, A. Amal Raj, R. Reghunathan, I.H. Joe, V.S. Jayakumar, J. Raman Spectrosc. 37 (2006) 1381.
- [38] J.N. Liu, Z.R. Chen, S.F. Yuan, J. Zhejiang Univ. Sci. B 6 (2005) 584.
- [39] M. Szafran, A. Komasa, E. Bartoszak-Adamska, J. Mol. Struct. 827 (2007) 101.
- [40] E. Kavitha, N. Sundaraganesan, S. Sebastian, M. Kurt, Spectrochim. Acta A Mol. Biomol. Spectrosc. 77 (2010) 612.